

Direct Numerical Simulation of Airfoil Separation Control Using a Synthetic Jet

W. Zhang and R. Samtaney

Physical Sciences and Engineering Division, King Abdullah University of Science and Technology,
4700 KAUST, Thuwal 23955-6900, Jeddah, Saudi Arabia

Abstract

Direct numerical simulations (DNS) are performed on a synthetic jet based separation control of flow over a NACA-0018 airfoil, at 10 degrees angle of attack and Reynolds number of 10^4 based on the airfoil chord length C and uniform inflow velocity U_0 . The actuator of the synthetic jet is simplified as a spanwise slot on the airfoil leeward surface with a wall-normal Poiseuille-type velocity profile and is positioned just upstream of the leading edge separation point. The momentum coefficient of the jet is chosen at a small value 2.13×10^{-4} normalized by that of the inflow, and two values of the reduced frequency $F^+ = fC/U_0 = 1.0$ and 4.0 are investigated. The DNS are conducted with an energy conservative spatially fourth-order parallel code solving the incompressible Navier-Stokes equations on a generalized curvilinear grid. We report results from both two- and three-dimensional simulations. The objectives of the present study are twofold: the first is to identify the effects of geometric variation introduced by the jet on the flow separation patterns; the second is to investigate the effects of synthetic jet on the separation control of flow over an airfoil, with the emphasis on the improvement of aerodynamic performance and related flow separation patterns. Numerical results reveal that the two-dimensional simulations significantly overpredict the lift and drag coefficients compared with the three-dimensional DNS due to differences in the prediction of separation. The geometric variation introduced by the actuator is confirmed to have statistically negligible effects on the flow separation. At proper pulsating frequency, the introduction of the synthetic jet greatly reduces the scope and duration of the separation bubble, increases the lift and may decrease the drag, thus improving the aerodynamic performance.

Introduction

Laminar flow separation at low Reynolds number significantly deteriorates the aerodynamic performance of an airfoil. Separation control is intended to delay and minimize the occurrence of separation, provide improved lift-to-drag ratio and consequently better economic performance in aerospace related applications. Periodic forcing using a synthetic jet (zero-net-mass-flux jet) is designed to reduce the separation by directly energizing the boundary layer flow, and introducing high kinetic energy flow from exterior to the boundary layer through the formation of vortices. The synthetic jet is preferred over conventional steady blowing in that it could achieve the same prescribed improvement with a much smaller momentum coefficient, sometimes up to a saving of two orders of magnitude. The actuators required could be small and light, and independent of the main propulsive system, which makes it a competitive candidate in future engineering applications.

The application of the synthetic jet in airfoil separation control has been studied both numerically [4, 7] and experimentally [1], and some general consensus has been reached regarding parameter choices and their effects. The synthetic jet is more effective when positioned just upstream of the separation point compared with the position within the separation bubble [4], and the pulsating frequency of the jet is usually close to the natural fre-

quency of the uncontrolled case. Although it has not been systematically investigated for the synthetic jet, studies on pulsed blowing jet find that the exit velocity with a proper skew angle could further improve the control effects by generating streamwise vortices that enhance the momentum transfer between the fluid inside and outside of the boundary layer [2, 5].

Laminar flow separation over an airfoil at low Reynolds number and relatively large angle of attack (stall or post-stall) is usually accompanied by separated shear layer transition. The breakdown from larger to smaller vortices changes the flow pattern in the boundary layer and consequently the aerodynamic performance of the airfoil. The application of a synthetic jet requires a deeper understanding of the flow separation and transition mechanisms. The present study performs direct numerical simulations (DNS) of flow over an airfoil with and without the separation control by a synthetic jet. The objectives of the present study are twofold. The first is to identify the effects of geometric variation introduced by the actuator on the flow separation patterns. Although the width of the jet is normally small, drilling an orifice or a slot on the airfoil surface changes the profile by introducing a discontinuous junction between the jet exit and the remaining smooth surface of the airfoil. This discontinuity may trigger artificial separation and its effects are usually mixed with those of the jet and have not been explicitly distinguished. The second is to investigate the effects of the synthetic jet on the separation control of flow over an airfoil, with the emphasis on the improvement of aerodynamic performance and related separation patterns. Qualitative and quantitative results are presented for reference for problems defined with similar configurations and parameters.

We perform both 2D and 3D DNS for four cases. The first is the baseline (uncontrolled) case, in which the airfoil profile is kept at its original state and no control technique is applied. The second is the zero-jet case; an orifice (2D) or a slot (3D) is put on the airfoil leeward surface but no blowing/suction is applied. This case is used to comparably identify the effects of geometric variation introduced by the actuator. The third and fourth cases are controlled cases: the synthetic jet is applied for separation control at two reduced frequencies, a low frequency at $F^+ = fC/U_0 = 1$ and a high frequency at $F^+ = 4$.

Physical Setup and Numerical Details

The airfoil chosen in this study is the NACA-0018 profile, shown in figure 1. The airfoil is assumed to be straight, i.e. without spanwise variation for the 3D DNS. The angle of attack is 10 degrees. The Reynolds number is fixed at $Re_c = 10^4$ based on chord length C and uniform incoming flow velocity U_0 . The profile of the airfoil is not modified for the baseline (uncontrolled) case, while an actuator is put at the leeward surface close to the leading edge for the zero-jet and controlled cases. The actuator of the jet is simulated as a simple orifice for the 2D simulation and a spanwise slot for the 3D simulation. The exit of the jet is denoted as a straight dashed line compared with the smooth curve of the remaining airfoil surface (see inset in figure 1).

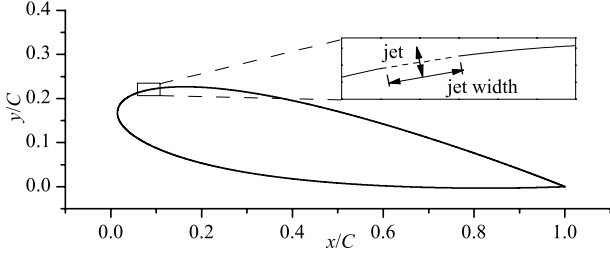


Figure 1. Geometric configuration of the airfoil and the jet.

There are several geometric and operational parameters for the synthetic jet, including the position $x^+ = x_{\text{jet}}/C$ and width $w^+ = \text{width}/C$, the reduced frequency of the time-varying jet $F^+ = fC/U_0$, and the profile and direction of the jet velocity. Because it is practically impossible to cover the whole parameter space, due to the expense involved in the DNS (about 3 million core-hours per case), in the present study we mainly focus on the effects of the frequency and choose fixed values for other parameters. The actuator is positioned at a short distance upstream of the time-averaged leading edge detachment point of the baseline case for better control effect, with its center located at $x_{2D}^+ = 0.08$ and $x_{3D}^+ = 0.13$. The width of the jet is $w^+ = 0.02$ and is resolved by 24 grid points. The direction of the jet is assumed to be normal to the local surface and no spanwise component is considered, and the velocity profile is of Poiseuille-type as follows:

$$u_{\text{jet}}(r,t) = u_{\text{max}} \left[1 - \left(\frac{r}{\text{width}/2} \right)^2 \right] \sin(2\pi ft), \quad (1)$$

$$-\text{width}/2 \leq r \leq \text{width}/2, \quad (2)$$

in which the maximum velocity $u_{\text{max}} = 0.2U_0$ and r is the distance to the jet center. The momentum coefficient is:

$$C_\mu = \frac{\int \int \rho U_{\text{jet}}^2 dr dz dt}{\rho U_0^2 C L_z / f} = 2.13 \times 10^{-4} \quad (3)$$

The computational domain is extended to ensure that the nearest exterior boundary is at least $10C$ away from the airfoil surface, and for 3D simulation the spanwise domain size is $L_z = C$. A C-type $2048 \times 256 (\times 128)$ mesh is used for all 2D (3D) simulations with the grids clustered near the airfoil. For all simulations the maximum Δy^+ is about 0.6, and maximum Δx^+ and Δz^+ are around 5.0 and 20.0. The time step size is about 2.0×10^{-4} . For 2D cases the simulation first runs for $100C/U_0$ and then for another $100C/U_0$ for the statistics, for 3D cases the two values are, respectively, $70C/U_0$ and $50C/U_0$.

The incompressible Navier-Stokes equations are solved by a semi-implicit solver based on fractional step method [8]. The Adams-Bashforth scheme is used for time marching. The spatial discretization is an energy conservative fourth-order scheme [3]. The pressure Poisson equation is solved by a multigrid solver with line-relaxed Gauss-Seidel method served as solver and smoother. The code is parallelized with standard MPI protocol and the computations are conducted on KAUST Shaheen (IBM Blue Gene-P) using up to 2,048 cores.

A uniform flow $(u, v, w) = (U_0, 0, 0)$ is imposed at the inflow boundary. At the outflow plane the convective outflow condition is used. No-slip boundary condition for velocity is prescribed on the airfoil surface. In 3D simulations periodic boundary condition is employed in the spanwise direction.

Results and Discussions

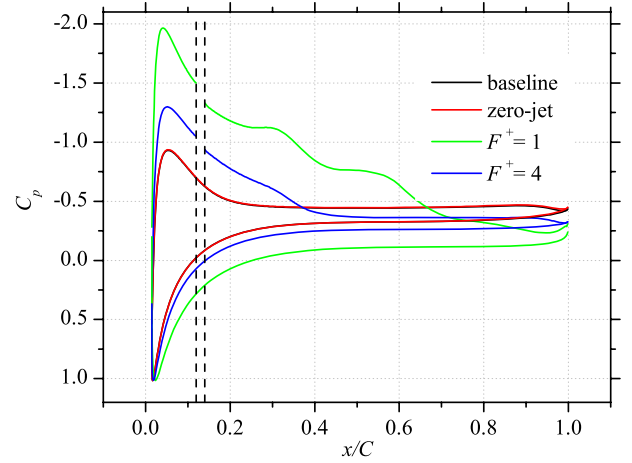


Figure 2. Time-spanwise-averaged pressure coefficient distributions on the leeward surface in 3D simulations. The vertical dashed lines denote the position of the actuator.

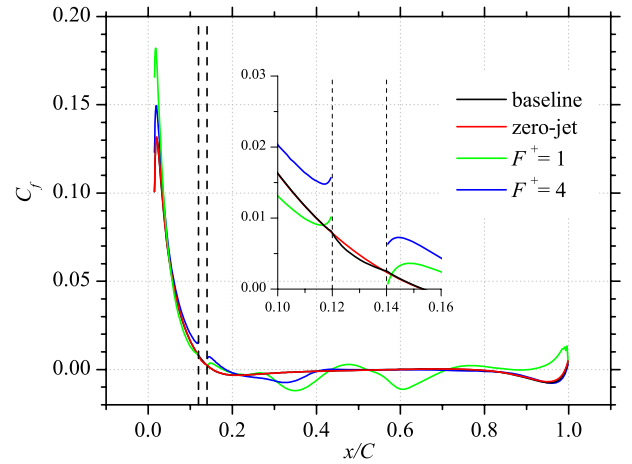


Figure 3. Time-spanwise-averaged skin friction coefficient distributions on the leeward surface in 3D simulations. The vertical dashed lines denote the position of the actuator.

The improvement in aerodynamic performance introduced by the synthetic jet is seen in tables 1 and 2 which list the lift and drag coefficients and lift-to-drag ratio for all four cases, as well as their improvements with respect to the baseline case. In both 2D and 3D simulations, the quantitative results of the zero-jet case show that the geometric variation on the airfoil surface introduced by the actuator has a negligible effect on the aerodynamic performance. The tiny differences between the results of baseline and zero-jet cases should mainly be attributed to the limitations of the simulations, including the resolution, the local mesh variation and the time interval used for statistics. By introducing the synthetic jet, the lift just increases slightly at $F^+ = 1$ while decreases a lot at $F^+ = 4$, but the drag in both two controlled cases decrease to almost half of the baseline value. However, the application of the synthetic jet as a separation control technique would not always be effective unless proper parameters are chosen. In the present study where the frequency is of interest, it is seen in Table 1 that a rapidly pulsating jet improves neither the lift nor the lift-to-drag ratio.

The 3D DNS relieve the two-dimensionality assumption and are expected to be closer to physical reality and hence more accurate and reliable. Some general conclusions can be drawn,

Case	Actuator	u_{jet}/U_0	F^+	C_l	C_d	C_l/C_d	$\Delta C_l(\%)$	$\Delta(C_l/C_d)(\%)$
1	No	-	-	0.7977	0.2205	3.6177	-	-
2	Yes	0.0	-	0.7975	0.2201	3.6234	-0.03	0.16
3	Yes	0.2	1.0	0.8643	0.1266	6.8270	8.35	88.71
4	Yes	0.2	4.0	0.4296	0.1230	3.4927	-46.15	-3.46

Table 1. Time-averaged lift and drag coefficients for 2D simulation.

Case	Actuator	u_{jet}/U_0	F^+	C_l	C_d	C_l/C_d	$\Delta C_l(\%)$	$\Delta(C_l/C_d)(\%)$
1	No	-	-	0.2536	0.1316	1.9210	-	-
2	Yes	0.0	-	0.2570	0.1328	1.9352	1.34	0.74
3	Yes	0.2	1.0	0.7880	0.1239	6.3600	210.73	230.08
4	Yes	0.2	4.0	0.3660	0.1091	3.3547	44.32	74.63

Table 2. Time-averaged lift and drag coefficients for 3D simulation.

which are in accordance with the 2D cases. The geometric variation brought by the actuator has no notable effects to the results, and the synthetic jet could improve the aerodynamic performance. There are also remarkable differences between the 2D and 3D results. The first is the difference of the lift and drag coefficients in the baseline and zero-jet cases. It is obvious that the 2D simulation overpredicts both two quantities due to incorrect prediction of separation, as also demonstrated by Gross and Fasel [2]. The second is that the synthetic jet operated at both two frequencies yields improved results. Unlike its 2D counterpart at $F^+ = 1$ where the lift is increased and the drag is substantially decreased, these quantities in 3D controlled cases do not show similar trends but are getting close to the 2D values, which indicates that three-dimensionality effects are weakened. This is attributed to the lock-in phenomenon, in which the vortices are shed at the frequency of the excitation. Since the actuator is simulated by a spanwise slot in this study, the flow field in the streamwise and wall-normal plane is locked to the excitation and this locking is spanwise the same, resulting a quasi-2D flow field.

Figure 2 shows the distribution of pressure coefficient along the airfoil surface. The introduction of the synthetic jet close to the leading edge respectively increases and decreases the wall pressure on the lower and upper side of the airfoil, which is the main reason for the lift improvement. For the baseline case, the pressure gradient in the middle of the leeward surface and downstream part is almost zero, while there is strong adverse pressure gradient (APG) for the controlled cases. Normally the APG is related to flow separation, especially close to the leading edge, but the emergence of separation bubble is also determined by the kinetic energy of the boundary layer flow. The flow is more resistant to the APG if the streamwise velocity is larger. In figure 3 we find that although the velocity direction of the jet is normal to the local surface, the jet slightly increases the wall-tangent velocity downstream of the slot. However, the jet at $F^+ = 1$ presents notably negative C_f in the middle of the airfoil, reflecting strong but not necessarily large separation in this region. This is demonstrated in figure 4. The streamwise velocity profiles are plotted at several streamwise stations. The size of the separation bubble above the airfoil leeward surface could be clearly distinguished by the negative streamwise velocity. For all cases the separation is definitely observed at $x/C = 0.2$ and it may occur upstream of this position. For the baseline case we observe that the separation bubble is large enough to cover most of the leeward surface, and its size in the wall-normal direction is also larger. The separation bubble extends to $y/C = 0.16$ at the trailing edge position. For the controlled cases, although the boundary layer flow detaches as early as at $x/C = 0.2$, the wall-normal size of the separation bubble is remarkably small (e.g. $0.025C$ at $x/C = 0.6$ for $F^+ = 1$), and it can not even be

observed downstream of $x/C = 0.7$ for the case of $F^+ = 1$.

The flow separation pattern can be quantitatively analyzed from the perspective of reverse flow close to the surface. We define the skin friction coefficient to be negative if the fluid is moving from downstream to upstream direction, which reflects separation. Inspired by the work of Simpson [6] for characterizing the steady free-stream separating turbulent boundary layers, here we define the quantity γ as the fraction of time that local C_f is positive:

$$\gamma = \frac{\int_{C_f \geq 0} dt}{\text{Total time}} \quad (4)$$

The streamwise distributions of γ are shown in figure 5. For the uncontrolled baseline and zero-jet cases, the flow steadily separated at around $x/C = 0.15$ and separation bubble is formed downstream of this position until the trailing edge. The synthetic jet does not eliminate separation nor push the separation point downstream, but it greatly alleviate the separation downstream of the actuator. In the case of $F^+ = 1$, the value of γ is normally larger than the uncontrolled cases, meaning that the fluid is relatively more prone to move from upstream to downstream and the separation is smaller in scope and shorter in duration.

The streamwise distributions of peak turbulent kinetic energy (T.K.E.) are shown in figure 6. For the baseline case the transition is notably observed at around $x/C = 0.5$ and the maximum value of T.K.E. occurs downstream of the trailing edge. For the two controlled cases, the flow is locked-on to the excitation imposed by the synthetic jet and the velocity components are fluctuating at the excitation frequency, hence the stochastic fluctuation due to the turbulent flow is remarkably suppressed. The peak values of T.K.E. for the $F^+ = 1$ case is much smaller than that of the $F^+ = 4$ case downstream of $x/C = 0.7$, reflecting that characteristic natural frequency the flow is close to $F^+ = 1$ and it is well locked-in in this case.

Conclusions

DNS are performed to investigate the effects of synthetic jet in the separation control for flow over an isolated NACA-0018 airfoil. The jet is located slightly upstream of the time-averaged leading edge separation point. Both 2D and 3D simulations are conducted and four cases are considered, including the uncontrolled baseline case, the zero-jet case and the controlled cases at two different frequencies. The results show that the 2D simulations overpredict both lift and drag coefficients due to incorrect separation prediction. The geometric variation brought by the actuator does not have statistically meaningful effects on the aerodynamic performance. By introducing the synthetic jet, the flow separation on the airfoil leeward surface is greatly alleviated both in scope and duration; the flow is locked to the pulsat-

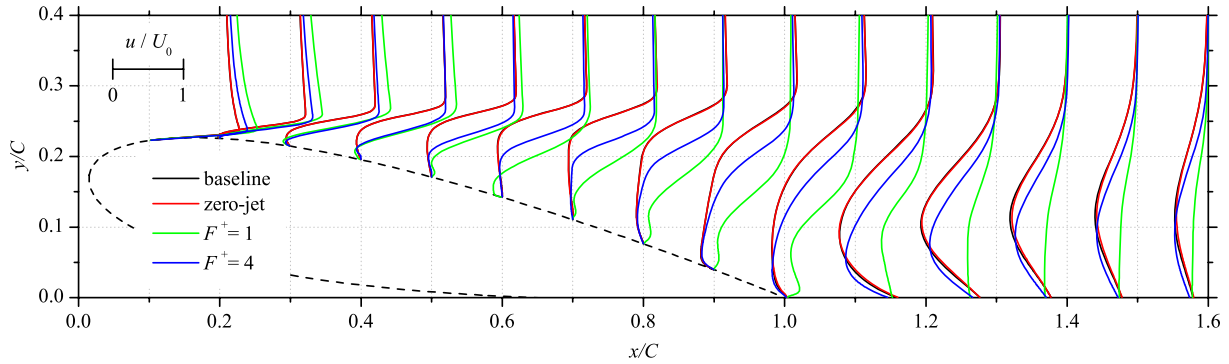


Figure 4. Time-spanwise-averaged streamwise velocity profiles in 3D simulations. The profiles are plotted at $x/C = 0.1, 0.2, \dots, 1.5$.

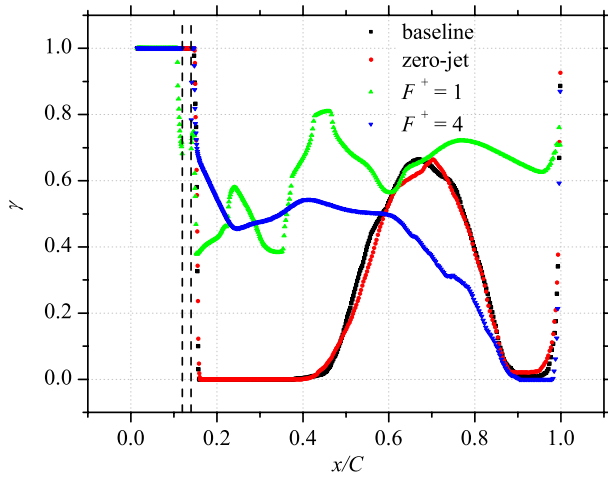


Figure 5. Streamwise distributions of γ on the leeward surface. The vertical dashed lines denote the position of the actuator.

ing jet and the flow field remains close to two-dimensional. The performance of the synthetic jet is determined by the choice of its frequency; a jet pulsating at high frequency gives less aerodynamic performance improvements than that at low frequency.

Acknowledgements

The work is supported by KAUST OCRF funded CRG project on simulation of turbulent flows over bluff bodies and airfoils. The IBM Blue Gene/P Shaheen at KAUST was utilized for the simulations.

References

- [1] Buchmann, N. A., Atkinson, C. and Soria J., Influence of ZNMF Jet Flow Control on the Spatio-Temporal Flow Structure Over a NACA-0015 Airfoil, *Exp. Fluids*, **54**, 2013, 1485(1-14).
- [2] Gross, A. and Fasel, H. F., Active Flow Control for NACA 6-series Airfoil at $Re=64,200$, *AIAA J.*, **48**, 2010, 1889-1902.
- [3] Morinishi, Y., Lund, T. S., Vasilyev, O. V. and Moin P., Fully Conservative Higher Order Finite Difference Schemes for Incompressible Flow, *J. Comput. Phys.*, **143**, 1998, 90-124.

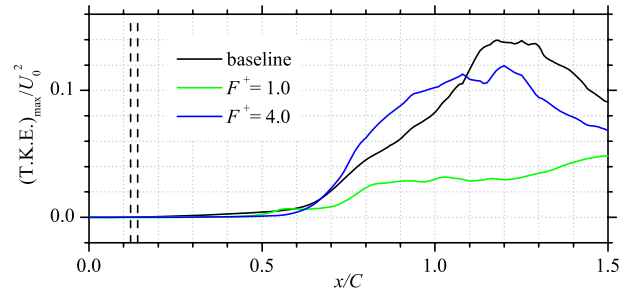


Figure 6. Streamwise distributions of peak time-spanwise-averaged turbulent kinetic energy $T.K.E.=\overline{u'u'+v'v'+w'w'}/2$. The dashed lines indicate the position of the actuator.

- [4] Raju, R., Mittal, R. and Cattafesta, L., Dynamics of Airfoil Separation Control Using Zero-Net Mass-Flux Forcing, *AIAA J.*, **46**, 2008, 3103-3115.
- [5] Shan, H., Jiang, L., Liu, C. Q., Love, M. and Maines, B., Numerical Study of Passive and Active Flow Separation Control Over a NACA0012 Airfoil, *Comput. Fluids*, **37**, 2008, 975-992.
- [6] Simpson, R. L., A Review of Some Phenomena in Turbulent Flow Separation, *J. Fluids Eng.*, **103**, 1981, 520-533.
- [7] You, D. and Moin, P., Active Control of Flow Separation Over an Airfoil Using Synthetic Jets, *J. Fluids Struct.*, **24**, 2008, 1349-1357.
- [8] Zang, Y., Street, R. L. and Koseff, J. R., A Non-staggered Grid, Fractional Step Method for Time-dependent Incompressible Navier-Stokes Equations in Curvilinear Coordinates, *J. Comput. Phys.*, **114**, 1994, 18-33.